AN EXPERIMENTAL STUDY ON MICRO-SCALE FLOW BOILING HEAT TRANSFER

Cristiano Bigonha Tibiriçá, Gherhardt Ribatski

Departament of Mechanical Engineering, Escola de Engenharia de São Carlos, University of São Paulo, Av. Trabalhador São Carlense, 400, São Carlos, SP, Brazil

ABSTRACT

In this paper, new experimental flow boiling heat transfer results in micro-scale tubes are presented. The experimental data were obtained in a horizontal 2.32 mm I.D. stainless steel tube with heating length of 464 mm, R134a as working fluid, mass velocities ranging from 50 to 600 kg/m^{2}s, heat flux from 5 to 55 kW/m^2, exit saturation temperatures of 22, 31 and 41 ^{o}C, and vapor qualities from 0.05 to 0.98. Flow pattern characterization was also performed from images obtained by high speed filming. Heat transfer coefficient results from 2 to 14 kW/m^{2}K were measured. It was found that the heat transfer coefficient is a strong function of the saturation pressure, heat flux, mass velocity and vapor quality. The experimental data were compared against the following micro-scale flow boiling predictive methods from the literature: Saitoh *et al*., Kandlikar, Zhang *et al*. and Thome *et al*. Comparisons against these methods based on the data segregated according to flow patterns were also performed. Though not satisfactory, Saitoh *et al*. worked the best and was able of capturing most of the experimental heat transfer trends.

INTRODUCTION

Flow boiling heat transfer inside channels having hydraulic diameters less than 3mm, identified here as micro-scale channels, has been studied since the late 1950s [1], but only in recent years it has turned into a major research topic in the thermal fluid science field. Most of this interest is driven by the industrial demand for compact devices capable of dissipating extremely high heat fluxes such as those expected for the next microprocessor generation. Despite of the enormous benefits that can be achieved by using precise designing methods, they are still not available and flow-boiling based heat-spreaders are been developed based on prototype machining and testing. In the last decade great effort has been put into identifying the main parameters governing micro-scale flow boiling heat transfer and also into quantifying their relevance.

In macro-scale flow boiling, different heat transfer mechanisms are dominant according to the vapor quality range, and heat flux and mass velocity levels. At low vapor qualities, nucleate boiling effects prevail while at high vapor qualities and prior to the liquid dryout, the heat transfer coefficient is mainly controlled by convective effects. The predominance of these mechanisms is commonly considered [2-7] when developing flow-boiling heat transfer coefficient predictive methods. Chen [2] was one of the pioneers of such an approach according to which the flow boiling heat transfer coefficient is calculated as follow:

$$h_{tp} = S \cdot h_{nb} + F \cdot h_{sp} \tag{1}$$

where h_{nb}, is given according to Foster and Zuber [8] nucleate pool boiling correlation, and h_{sp} is the liquid single-phase heat transfer coefficient calculated according to Dittus-Boelter [9] correlation. In Eq. (1) S is the nucleate boiling suppression factor that takes into account steeper temperature gradients near the wall due to the fluid motion which tends to suppress the number of bubble active sites. The convective enhancement factor, F, takes into account the increment of convective effects, relative to that of the single-phase flow of the liquid, promoted by the flow acceleration due to the evaporation process. Since its proposal, several authors have adjusted their database to Chen's type correlations. This approach has been also adopted for micro-scale flow boiling.

Liu and Winterton [3] developed a method to predict saturated and subcooled flow boiling heat transfer based on Chen's basic hypothesize that both convective and nucleate boiling heat transfer mechanisms play a role in flow boiling. In their method, the convective and nucleate boiling contributions were added according to a power-type asymptotic approach with an exponent of 2. They adjusted their method according to a database that comprises more than 5000 experimental data points, nine fluids and tube internal diameters ranging from 2.92mm to 32mm.

The micro-scale flow-boiling predictive method by Kandlikar and Balasubramanian [4] is just a modified version of the previous method for conventional channels developed by Kandlikar [10] in the early 1990'. The main modifications are related to the fact that laminar flows were taken into account and gravitational effects were neglected. The values for the empirical constant characteristic of the fluid/surface-material pair were kept the same as in the previous version. Zhang *et al.* [5] have modified the Chen method in order to predict micro-scale flow boiling heat transfer. In their approach, the correlation by Foster and Zuber [8] was maintained to predict the nucleate boiling heat transfer component. The boiling suppression factor proposed by Chen was also retained. Then, to determinate the convective enhancement factor and the single-phase heat transfer coefficient, vapor and liquid flow conditions (laminar or turbulent) were taken into account. Their method was compared against independent experimental data from the literature for water, R11, R12 and R113. Saitoh *et al*. [6] by modifying the macro-scale flow boiling correlation by Chen and using a database comprising only R134a experimental results proposed a model which covers both macro- and

micro-scale flow boiling heat transfer. In his method, emphasize was exercised in order to properly capture the tube diameter effect on the heat transfer coefficient through the Weber number. Empirical coefficients were adjusted by them based on a database consisting of tube diameters ranging from 0.51 mm to 11.0 mm. Recently, Bertsch *et al.* [7] have proposed a Chen type predictive method based only on micro-scale flow boiling data which includes 3899 experimental data points covering 12 fluid and hydraulic diameters ranging from 0.16 to 2.92 mm.

Thome *et al.* [11] have developed a micro-scale model that describes the heat transfer processes during the cyclic passage of elongated bubbles in a micro-scale channel. In this model, a time-averaged local heat transfer coefficient is obtained during the cyclic passage of (i) a liquid slug, (ii) an evaporating elongated bubble, and (iii) a vapor slug when present. The model includes five experimental parameters obtained by Dupont *et al.* [12] according to an experimental database with 1591 data taken from seven independent studies in the literature.

To evaluate the ability of the available methods to predict heat transfer coefficients in micro-scale channels, Tibiriçá *et al.* [13] have compared 7 heat transfer predictive methods [3-7,11] against a database comprising 15 fluids and containing more than 2500 micro-scale flow boiling experimental data points from the literature. They found that the flow boiling heat transfer methods poorly predict the database; however, they also indicated that such result was not surprising since large discrepancies between data from different authors were observed.

Several aspects contribute for the huge discrepancies among experimental databases. Firstly, quite a large number of studies were performed in the presence of thermal instabilities which effects may affect drastically the heat transfer trends as shown by Consolini [14]. Experimental characteristics as the internal surface roughness of the channels are rarely mentioned, consequently, database comparisons are performed and heat transfer trends are suggested without an adequate knowledge of the experimental conditions. Moreover, erroneous data regression procedures are frequently adopted as shown by Ribatski *et al*. [15]. Inherent difficulties verified in conventional flow boiling heat transfer measurements are incremented in the case of micro-scale conditions due to the reduced scales involved. Energy balances under single-phase flow conditions and single-phase flow heat transfer measurements in order to validate the experimental apparatus are not a common practice. Finally, even when using state-of-the-art instrumentation and calibration procedures, experimental heat transfer coefficient errors, most of the time higher than ±20% [14], still play an important role in the data analyses.

In this paper, new micro-scale flow boiling heat transfer results are presented. Extreme care was exercised in order to perform accurate heat transfer coefficient measurements. Flow boiling experiments were performed for R134a in a horizontal stainless tube with and internal diameter of 2.32 mm and 464mm long. The principle heat transfer trends were identified and discussed taking into account two-phase flow visualizations. The experimental results were compared against the leading micro-scale flow boiling predictive methods.

EXPERIMENTS

Test apparatus and experimental procedure

The experimental setup is comprised of refrigerant and ethylene-glycol circuits. The refrigerant circuit is shown schematically in Fig. 1. It globally comprises a micropump, to drive the working fluid through the circuit, a pre-heater, to establish the experimental conditions at the inlet of the test section, a test section, a visualization section, a condenser to condense the vapor created in the heated sections, and a reservoir. The water-glycol circuit (not shown) is intended to condense and subcool the fluid in the refrigerant circuit. The cooling effect is obtained by a 60% solution of ethylene glycol/water that operates as intermediate fluid in a system that comprises electrical heaters actuated by PID controllers, 3 water/glycol tanks, heat exchangers and a refrigeration circuit.

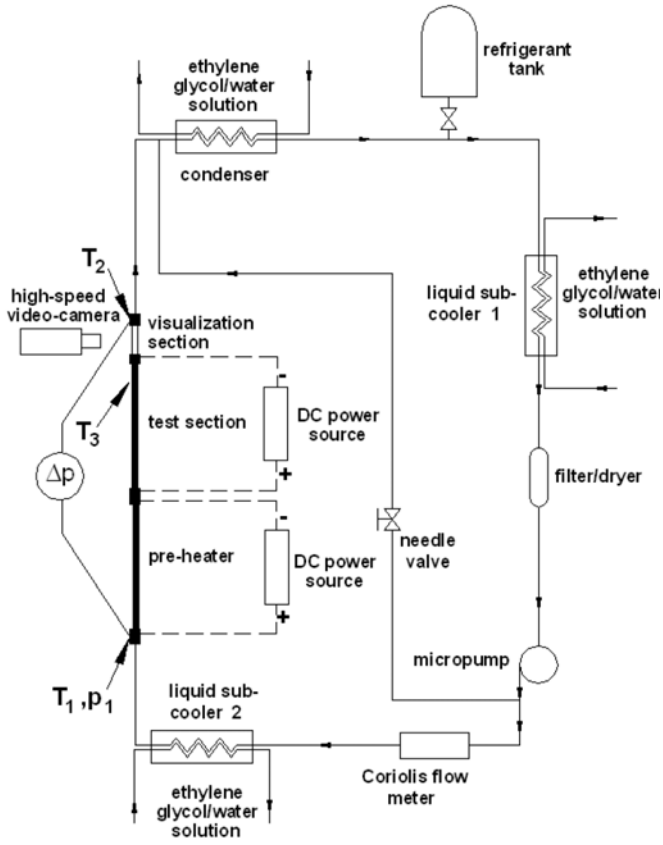

Figure 1. Schematic diagram of the refrigerant circuit.

In the refrigerant circuit, starting from the subcooler 1, the test fluid flows through the filter to the micropump (selflubricating without oil). Downstream the micropump, a bypass piping line containing a needle-valve is installed so that together with a frequency controller on the micropump the desired liquid flow rate can be set. There is then a Coriolis mass flow meter and the subcooler 2 to assure that the fluid entering the pre-heater is subcooled. Just upstream the pre-heater inlet, the enthalpy of the liquid is estimated from its temperature T_1 by a 0.25mm thermocouple within the pipe and its pressure p_1 by an absolute pressure transducer. At the pre-heater, the fluid is heated up to the desired condition at the test section inlet. The pre-heater and the test section are horizontal stainless steel tubes with an internal diameter of 2.32mm and 464mm long. Both are heated by applying direct

DC current to their surface and are thermally insulated. Their internal surface roughness was measured in terms of the CLA arithmetic average, *Ra*, and a value of 0.33μm was found. The power is supplied to the pre-heater and the test section by two independent DC power sources controlled from the data acquisition system. The visualization section is a horizontal fused silica tube with an inner diameter of 2.1mm, a length of 85mm, and is located just downstream to the test section. The pre-heater, the test section and the flow visualization section are connected through junctions made of electrical insulation material and specially designed and machined in such way to match up their ends and keep a smooth and continuous internal surface. Once the liquid leaves the visualization section its temperature T_2 is determined from a 0.25mm thermocouple within the pipe. The corresponding absolute pressure is estimated from a differential pressure transducer that gives the total pressure drop between the pre-heater inlet and the flow visualization section outlet, Δp. Then, the working fluid is directed to the tube-in-tube type heat exchanger where it is condensed and subcooled by exchanging heat with the anti freezing ethylene glycol aqueous solution. The refrigerant tank containing a serpentine coil operates as a reservoir of the working fluid and is used to control the saturation pressure in the refrigerant circuit. The saturation pressure is set by acting on the temperature of the anti freezing ethylene glycol aqueous solution that flows through the serpentine coil within the tank.

Wall temperatures are measured through 0.25mm type K thermocouples fixed along the test section. Rubber o-rings having an internal diameter smaller than the test section are used to fix the thermocouples on the surface by pressuring them against the tube wall. At each measuring cross-section, the surface temperature is read at three locations, 90° spaced, from the bottom to the top of the tube, as indicated in Fig. 2.

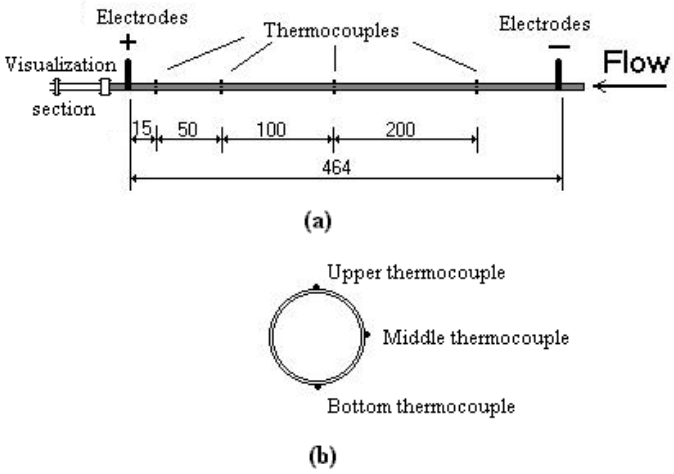

Figure 2. Details of the test section and thermocouples positioning along its surface.

The experiments were conducted first by setting the temperature in the refrigerant tank. This temperature is kept almost constant by a thermal-controller system. Once established the saturation pressure in the refrigerant circuit by controlling the temperature in the refrigerant tank, the mass velocity was set through a frequency controller acting on the micropump. Then, the desired experimental heat flux is imposed to the test section and by varying the power supplied to the pre-heater, experimental results for distinct vapor qualities, keeping the remaining parameters fixed, are obtained. Tests were conducted by gradually increasing the heat flux up. The datum points were logged only under steady-state conditions which were characterized by temperature measurement variations within 0.3K during at least 2 minutes.

During the thermocouple calibrations and the experimental campaign, the room containing the test facility had its temperature maintained about 22°C. Such a procedure was adopted in order to minimize possible effects of the room temperature variation on the measurements accuracy.

Data reduction

Heat transfer coefficient. Local heat transfer coefficients are calculated according to the Newton's cooling law as follow:

$$h_{local} = \frac{q}{T_w - T_{sat}(z)} \tag{2}$$

where T_w is the surface temperature of the inner tube wall estimated according to the Fourier's law based on the outer wall temperature measurements, and assuming both one-dimensional conduction and adiabatic external surface. T_{sat} is the local saturation temperature of the refrigerant. To estimate this temperature, firstly, based on the heat flux and on the measured temperature and pressure at the pre-heater inlet, the subcooled region length, the single-phase pressure drop over its length, and the saturation temperature at the beginning of the saturated region were calculated by solving simultaneously an equation of state relating p_{sat} and T_{sat} plus energy balance and single-phase pressure drop equations. The overall pressure drop over the saturated region is then determined by subtracting the single-phase pressure drop from the measured total pressure drop, Δp. After that, a constant pressure drop gradient given by the ratio of the overall pressure drop over the saturated region and its length is assumed from the beginning of the saturated region until the end of the flow visualization section. After that, T_{sat} is calculated from the estimated local saturation pressure. The heat flux, q, is calculated as the ratio between the electrical power supplied to the test section and its internal area based on the heated length. The electrical power is given by the product between the electrical current and the voltage supplied by the DC power sources.

The perimeter-average heat transfer coefficient at each cross-section is calculated as follow:

$$\overline{h(z)} = \frac{h_{top}(z) + 2 \cdot h_{middle}(z) + h_{bottom}(z)}{4} \tag{3}$$

Vapor quality. The local vapor quality, $x(z)$ is obtained from energy balances over the pre-heater and the test section.

Experimental validation and uncertainties

Compressible volume instabilities also termed in the literature by "explosive boiling" (as in [16]) are a common phenomenon in micro-scale flow boiling. These instabilities can promote severe pressure and temperature oscillations in the flow and seems related to some of discrepancies observed when comparing experimental results from different authors (see Consolini *et al.* [17]). During the present experimental campaign, such instabilities were not observed and the fluctuations of the fluid temperature and pressure were within the uncertainty range of their measurements.

Single-phase flow experiments were performed in order to assure the accuracy of the estimated vapor quality and

evaluate the effective rate of heat transferred to the single phase refrigerant, *(ΔE/E)*, defined as follow:

$$\left(\Delta E/E\right) = \frac{\left(\left[\left(\pi D^2\right)/4\right] G\left(i_{out} - i_{in}\right)\right)}{P_1 + P_2} \quad (8)$$

where i_{in} and i_{out} are the refrigerant enthalpies estimated at the pre-heater inlet and just downstream the visualization section, respectively.

As one can see in Fig. 3, the heat losses decrease with increasing the mass velocity with an effective rate of heat transferred to the refrigerant lower than 10% for $G \geq 100 kg/m^2s$ and than 5% for $G \geq 400 kg/m^2s$. Reasonable heat losses are observed for $G = 50 kg/m^2s$.

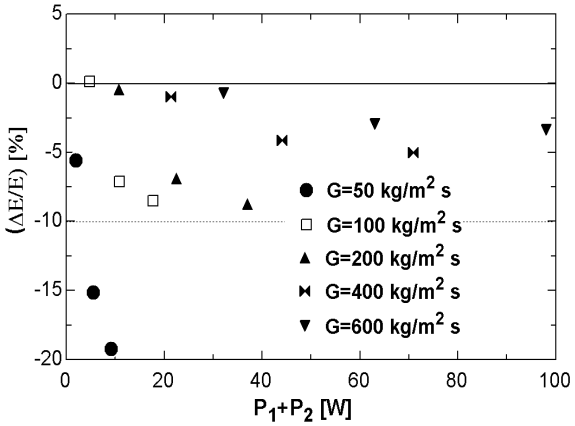

Figure 3. Evaluation of the effective rate of heat transferred to the single-phase flow refrigerant.

Temperature measurements were calibrated and the temperature uncertainty evaluated according to the procedure suggested by Abernethy and Thompson [18]. Accounting for all instrument errors, uncertainties for the calculated parameter were estimated using the method of sequential perturbation according to Moffat [19]. The experimental uncertainties associated with the sensors and calculated parameters are listed in Table 1. The experimental heat transfer coefficient error was always less than 30% with an average absolute error of 8.5% calculated based on the total of 2508 experimental data points obtained in this study.

In order to evaluate the accuracy of the measurements and validate the flow boiling results, single-phase heat transfer and pressure drop experiments were also performed and compared against the results provided by Gnielinski [20] and Petukhov [21] correlations, respectively. Figure 4 shows that the measured single-phase heat transfer coefficients agree reasonably well with those predicted by the correlation. Though not shown in this paper, good agreement was also obtained when comparing measured pressure drops against the predicted results.

Table 1. Uncertainty of measured and calculated parameters.

Parameter	Uncertainty	Parameter	Uncertainty
D	20 μm	*p*	4.5 kPa
L	1 mm	*Δp*	150 Pa
G	0.8%	P_1, P_2	0.88%
h	<30%	*T*	0.15 °C
x	<5%		

To double-check the measurements performed in this study, a comparison against previous flow boiling data from the literature under conditions somewhat similar to those in the present work is displayed in Fig. 9. In this figure, it is observed that the present data agree reasonably well with those by Yan and Lin [22]. These authors performed their experiments for R134a in a multi micro-channel test section composed by circular channels with internal diameters of 2.0mm.

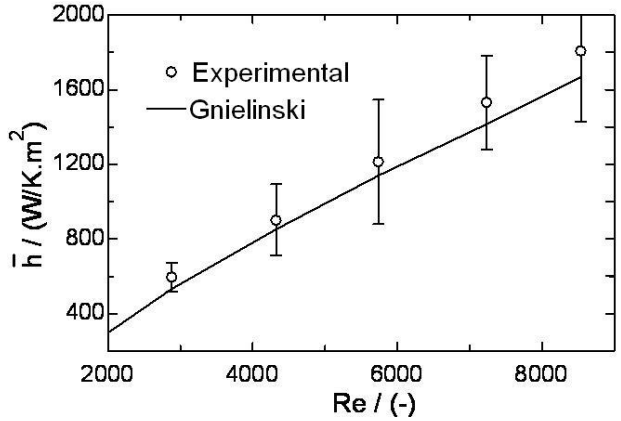

Figure 4. Comparison between the experimental single-phase heat transfer coefficient and the values predicted by Gnielinski [20] correlation (T_{exit}= 40°C).

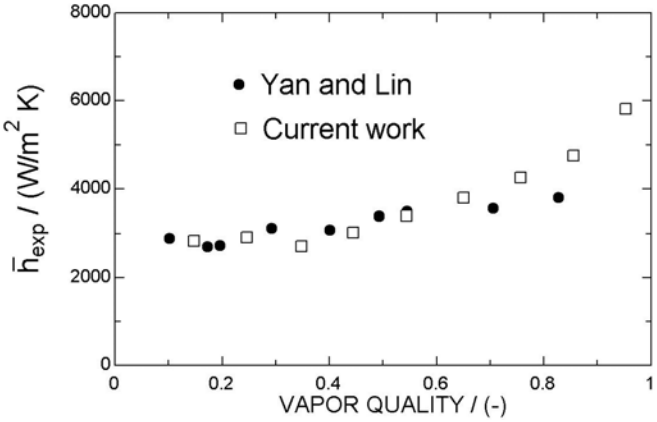

Figure 9. Comparison of the present flow boiling data against data from the literature [22] (G=200 kg/s.m^2, q=5kW/K.m^2, T_{sat}=31°C)

RESULTS

Heat transfer coefficient along the tube perimeter

Figure 5 shows the effect of the vapor quality on the heat transfer coefficient along the perimeter of the test section. Heat transfer coefficient measurements on the top, middle and bottom of the test tube for the thermocouples located 15mm far from the end of the heated region of the test section are displayed. Figure 5 also shows two-phase flow images corresponding to the heat transfer measurements. These images were obtained by high speed filming at the visualization section located just 50mm downstream the heat transfer measurements. According to this figure, stratification effects are present and a thicker liquid film is observed in the tube bottom region. This behavior affects the heat transfer coefficient as follow: (i) for vapor qualities up to 0.85, the heat transfer coefficient increases in the upward direction along the tube perimeter. This result is related to the lower thermal resistance in the upper part of the tube since the liquid film thickness decreases upwards as displayed in the

two-phase flow images; (ii) for vapor qualities higher than 0.85, the heat transfer coefficient decreases in the upward direction. Such a behavior permit infers the occurrence of a progressive surface dryout initiating from the upper part of tube with increasing vapor quality. It is important to highlight the fact that stratified flows were not detected during the current experimental campaign [23].

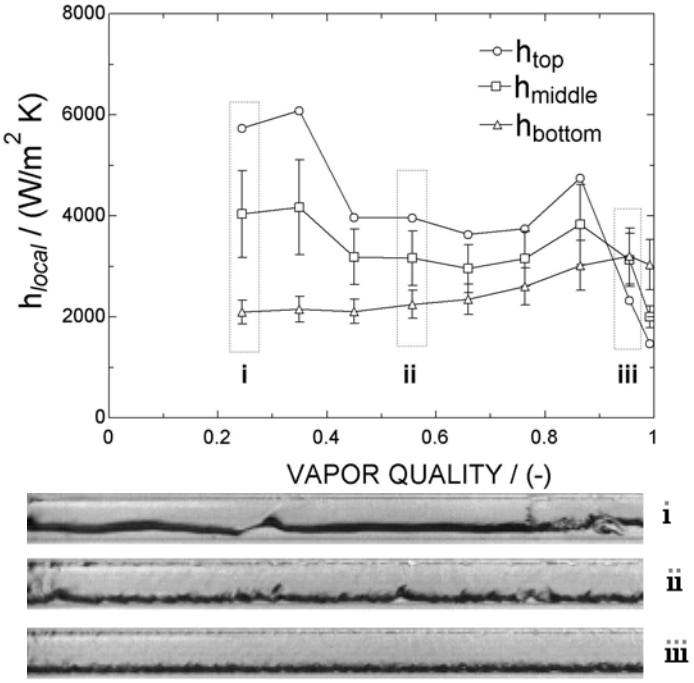

Figure 5. Heat transfer coefficient distribution along the tube perimeter and the corresponding two-phase flow images (G=100 kg/m^{2}s, q=5kW/m^2, T_{sat}=22^{o}C).

Parametric analyses of the experimental results

In this item, a parametric investigation of the effect of the experimental variables on the heat transfer coefficient is presented. In this analysis, only perimeter-average heat transfer coefficients defined according to Eq. (3) are considered.

Mass velocity. Figure 6 illustrates the effect of the mass velocity on the heat transfer coefficient for different heat flux levels and a saturation temperature of 31^{o}C. According to this figure, in general, the heat transfer coefficient increases with increasing mass velocity. This effect becomes more pronounced as the vapor quality increases. Distinct heat transfer behaviors with increasing vapor quality are observed according to a mass velocity threshold of 200kg/m^{2}s. For mass velocities higher than this threshold, the heat transfer coefficient increases with vapor quality until vapor qualities values up to 90% while for mass velocities lower than 200kg/m^{2}s the heat transfer coefficient presents a premature and smooth decrease with increasing vapor quality. The effects of mass velocity on the heat transfer behaviors are maintained independent of the heat flux level. A mass velocity threshold defining different heat transfer trends with vapor quality were also observed by Saitoh *et al*. [24] for his experimental data in a 3mm ID tube.

Saturation temperature. Figure 7 displays the effects of the saturation temperature on the heat transfer coefficient for different experimental conditions. It can be noted that in general the heat transfer coefficient increases with increasing saturation temperature. Such behavior is more pronounced at low vapor qualities and mass velocities and becomes almost negligible at high mass velocities and vapor qualities. These results are qualitatively in agreement with those data obtained for flow boiling in macro-scale channels. Thus, it is not surprising that macro-scale heat transfer prediction approaches as the one proposed by Chen [2] are adopted for micro-scale flow boiling and some of them seems work satisfactorily under such conditions when compared against its own database.

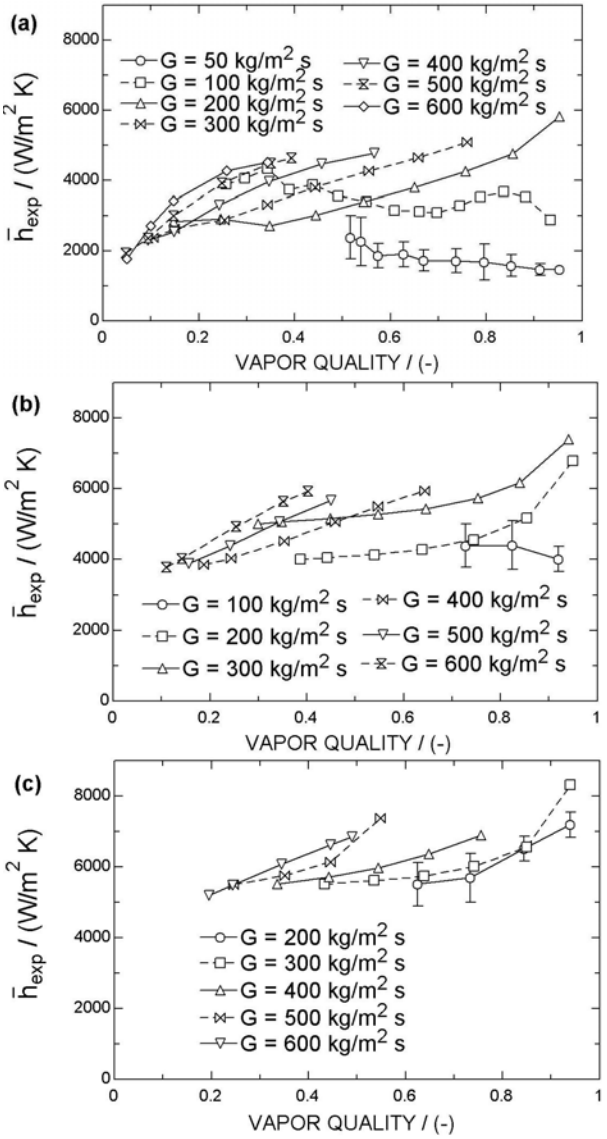

Figure 6. Illustration of the effect of the mass velocity on the heat transfer coefficient for different hat fluxes and T_{sat}=31^{o}C. (a) q=5kW/m^2; (b) q=15 kW/m^2; (c) q=25kW/m^2.

Heat flux. According to Figure 8, except for some of the results at vapor qualities higher than 0.9, the heat transfer coefficient increases with heat flux independently of the mass velocity range. Such behavior differs from that observed in macro-scale channels according to which the heat transfer coefficient increases with increasing the heat flux but only at low vapor qualities and mass velocities. Additionally, this behavior is related to the fact that nucleate boiling has been suggested as the dominant heat transfer mechanism in micro-scale channels. This statement comes from a misconception that an evaporation process dependent on the heat flux necessarily means that nucleate boiling is the controlling mechanism. Thome *et al*. [11], for elongated bubble flow, and

Mudawar *et al*. [25] for annular flow, have shown that the evaporation of a thin liquid film can also result that the heat transfer coefficient increases with heat flux.

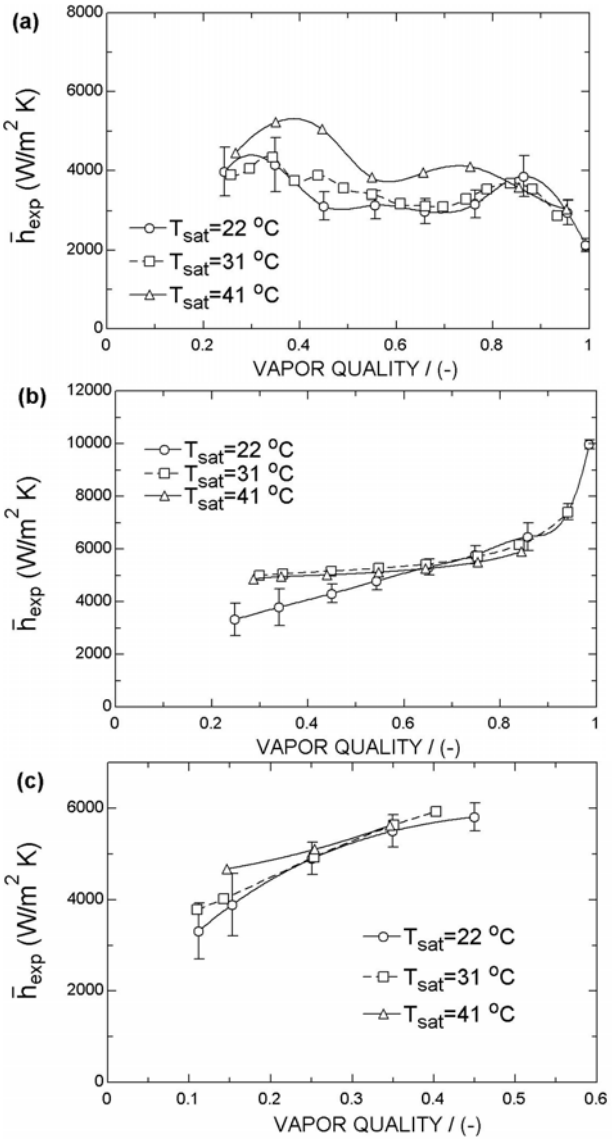

Figure 7. Illustration of the effect of the saturation temperature on the heat transfer coefficient. (a) G=100 kg/m^{2}s; q=5 kW/m^2 (b) G=300 kg/m^{2}s; q=15 kW/m^2 (c) G=600 kg/m^{2}s; q=5 kW/m^2

Comparison of the experimental data and the prediction methods

In order to evaluate the capability of the current flow boiling prediction methods to predict the present database, a comparison between the experimental data and six flow boiling heat transfer prediction methods [3-7,11] was performed. This comparison includes both macro- and micro-scale methods and a total of 2508 experimental data points with 627 of them having their flow pattern identified by high speed filming. The predictive methods are evaluated according to two criteria: the fraction of data predicted to within ±30%, λ , and the mean absolute error, ε.

Table 2 depicts the statistical comparisons of the methods for the overall database and also comparisons for the data segregated according to each flow pattern. Bubbly flows are not considered since they were observed only for calculated thermodynamic equilibrium vapor quality just above zero and, under this condition, saturated flow boiling conditions, the focus of this study, are not assured due to the vapor quality uncertainties. Bubbly flows are also expected at mass velocities higher than 700kg/m^{2}s, however such high flow rates are not achievable by the current experimental setup.

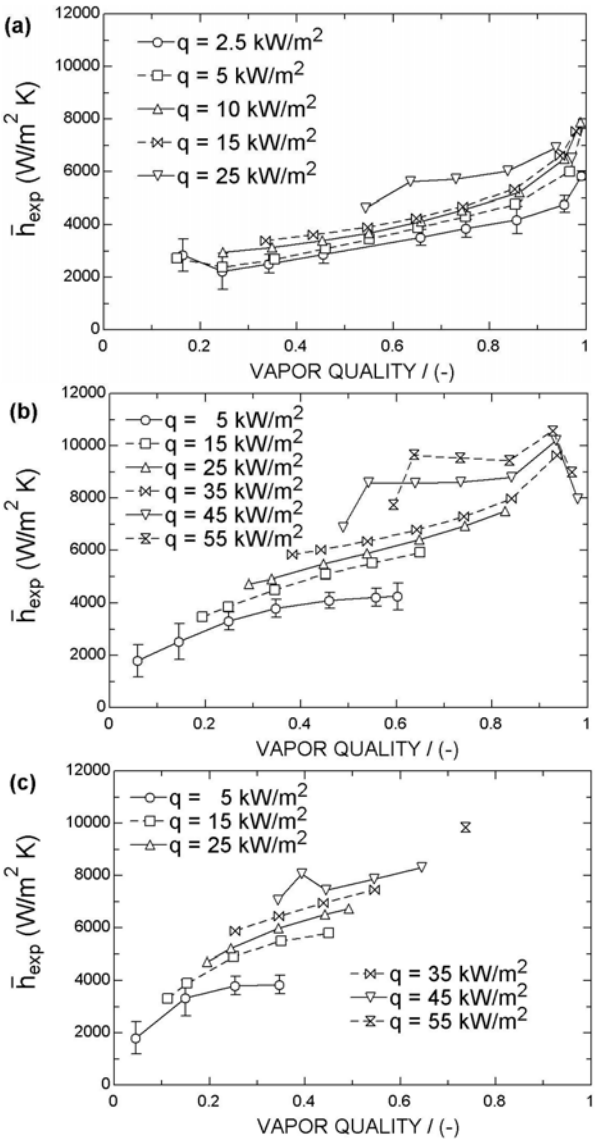

Figure 8. Illustration of the effect of the heat flux on the heat transfer coefficient for T_{sat}=22°C. (a) G=200 kg/m^{2}s; (b) G=400 kg/m^{2}s; (c) G=600 kg/m^{2}s

According to Table 2, Saitoh *et al.* [6] method worked the best when compared against the overall database. This result may be related to the fact that the empirical constants in their method were adjusted based solely on R134a data and for internal tube diameters ranging from 0.5mm to 11mm, so, coinciding with the experimental conditions of the present study. Saitoh *et al.* [6] method is also ranked as the best to predict flow boiling heat transfer under annular flow conditions. Bertsch *et al.* [7] provided the best heat transfer predictions for churn and elongated bubble flows.

A good predictive method should not be only statistically accurate, but should also be able of capturing the main trends of the experimental results. Taking it into account, Fig. 11 displays the evolution of the heat transfer coefficients vs. vapor quality in comparison to the heat transfer predictive methods for different experimental conditions. The heat transfer peak at low vapor qualities indicated by the 3-Zone model [11] seems to occur according to the experimental

results only in Fig. 11d containing the data obtained for the highest heat flux and mass velocity. Higher experimental heat transfer coefficients at lower vapor qualities are also displayed in Fig. 11b for G=50kg/m^{2}s, however, the heat transfer coefficient falloff with increasing mass velocity is much steeper than the one indicated by the 3-Zone model. Saitoh *et al*. [6] is the unique method predicting reasonably well the increase of the heat transfer coefficient with vapor quality at high vapor qualities that is displayed in Figs. 11b and 11c. The heat transfer coefficient discontinuities provided by Saitoh *et al*. [6] method are related to transitions from turbulent to laminar flow. The flow transition is based on the liquid Reynolds number and affects the convective heat transfer parcel of his method.

Table 2. Comparison between heat transfer prediction methods and the experimental database.

Flow pattern (n° of data points)		PREDICTIVE METHOD					
		Zhang *et al.*	Thome *et al.*	Kandlikar	Liu Winterton	Saitoh *et al.*	Bertscha *et al.*
Elongated bubbles (26)	ε	97.1	51.1	62.9	58.9	47.1	**37.8**
	λ	26.9	30.8	23.1	7.7	26.9	**38.5**
Churn (63)	ε	70.0	36.5	62.0	39.8	36.7	**25.4**
	λ	27.0	46.0	19.0	52.4	52.4	**81.0**
Annular (538)	ε	48.0	29.1	39.9	39.5	**22.5**	25.0
	λ	40.0	58.6	37.9	46.3	**75.8**	74.3
Overall database (2508)	ε	50.7	32.5	43.1	40.7	**23.7**	36.8
	λ	41.2	51.1	35.6	43.3	**73.5**	56.3

CONCLUSION

New accurate micro-scale flow boiling heat transfer data for R134a in a 2.32mm circular tube were obtained and presented. The experimental data was parametrically analyzed and compared against predictive methods. The conclusions can be summarized as:

1. Flow stratification was visualized and local wall temperature measurements revealed its effect on the circumferential variation of the heat transfer coefficient along the tube perimeter.
2. Generally speaking, the heat transfer coefficient increases with heat flux, mass velocity and saturation temperature. Distinct heat transfer behaviors with increasing vapor quality are observed according to a mass velocity threshold of 200 kg/m^{2}s.
3. The predictive method proposed by Saitoh *et al.* [6] worked the best and captured accurately the fact that under certain heat flux and mass velocity conditions the heat transfer coefficient increases with vapor quality at high vapor qualities.

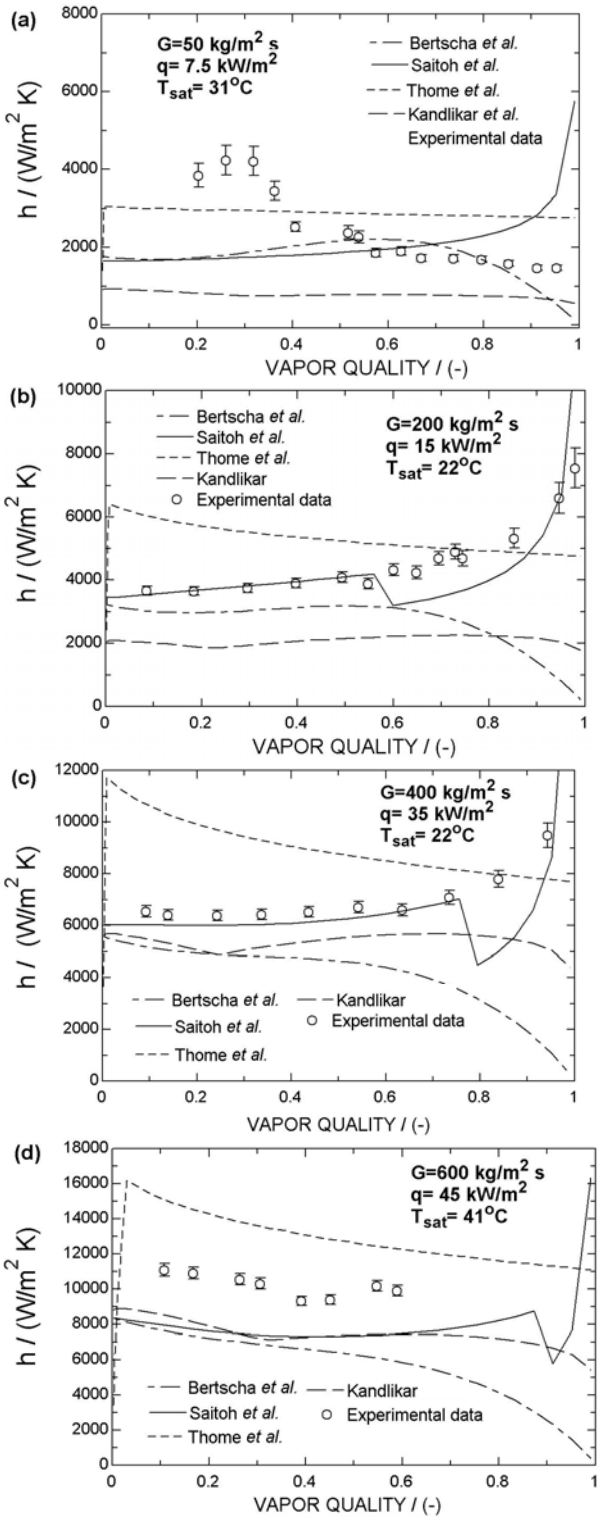

Figure 11. Heat transfer coefficient evolution with vapor quality according to the experimental data and predictive methods.

Acknowledgment

The authors gratefully acknowledge the financial support under contract numbers 05/60031-0, 06/52089-1 and 07/53950-5 given by FAPESP (The State of São Paulo Research Foundation, Brazil). The technical support given to this investigation by Mr. José Roberto Bogni is also appreciated and deeply recognized.

NOMENCLATURE

D	tube diameter, (m)
E	transferred energy to the tube (J)
G	mass velocity, (kg/m^{2}s)
h	heat transfer coefficient, (W/m^{2}K)
i	enthalpy (J/kg)
L	length, (m)
p	pressure, (Pa)
P	electrical power, (W)
q	heat flux (W/m^2)
Re	Reynolds number, (dimensionless)
T	temperature, (^{o}C)
x	vapor quality (-)
z	axial position (m)

Greek symbols

Δp	pressure drop

Subscripts

bottom	bottom of the tube
exp	*experimental*
local	at a specific position on the tube
middle	middle of the tube
nb	nucleated boiling
sp	single phase
top	top of the tube
tp	two-phase

REFERENCES

1. W. Lowdermilk, C. Lanzo, and L, Siegel, Investigation of boiling burnout and flow stability for water flowing in tubes, NACA. TN 4382, 1958.
2. J.C. Chen, Correlation for boiling heat transfer to saturated fluids in convective flow, *I&EC Process Des. Dev.*,vol. 5 (3), pp. 322–329, 1966.
3. Z. Liu and R. H. S. Winterton, A General Correlation for Saturated and Subcooled Flow Boiling in Tubes and Annuli, Based on a Nucleate Pool Boiling Equation, *Int. J. of Heat and Mass Transfer*, vol. 34, pp. 2759–2766, 1991.
4. S.G. Kandlikar, P. Balasubramanian, An extension of the flow boiling correlation to transition, laminar, and deep laminar flows in minichannels and microchannels, *Heat Transfer Eng.*, vol. 25, pp. 86–93, 2004.
5. W. Zhang, T. Hibiki, K. Mishima, Correlation for flow boiling heat transfer in mini-channels, *Int. J. Heat Mass Transfer*, vol. 47, pp. 5749– 5763, 2004.
6. S. Saitoh, H. Daiguji, H. Hihara, Correlation for boiling heat transfer of R-134a in horizontal tubes including effect of tube diameter, *Int. J. Heat and Mass Transfer*, vol. 50, pp 5215–5225, 2007.
7. S. Bertsch, A. Eckhard, Groll, Suresh, V. Garimella, A composite heat transfer correlation for saturated flow boiling in small channels, *Int. J. of Heat and Mass Transfer*, in press, 2008.
8. H. K. Foster and N. Zuber Bubble dynamics and boiling heat transfer. *AIChe Journal* vol.1, pp. 531-535, 1955.
9. F.W. Dittus and L. M. K. Boelter, Heat transfer in automobile radiators of the tubular type. University of California *Publications in engineering,* vol.2, pp. 443-461, 1930.
10. S. G. Kandlikar, A Model for Predicting the Two-Phase Flow Boiling Heat Transfer Coefficient in Augmented Tube and Compact Heat Exchanger Geometries, *J. Heat Transfer*, vol. 113, pp. 966–972, 1991.
11. J. R. Thome, V. Dupont and A. M. Jacobi, Heat Transfer Model for Evaporation in Microchannels, Part I: Presentation of the Model, *International Journal of Heat and Mass Transfer*, vol. 47, pp. 3375–3385, 2004.
12. V. Dupont, J.R. Thome, A.M. Jacobi, Heat transfer model for evaporation in microchannels. Part II: comparison with the database, *International Journal of Heat and Mass Transfer*,v. 47, p. 3387–3401, 2004.
13. C.B. Tibiriçá and G. Ribatski, Análise de Dados Experimentais e Métodos Para Previsão do Coeficiente de Transferência de Calor em Micro-Canais, in: Proceedings of the 1st *Brazilian Meeting on Boiling, Condensation and Multiphase* Flow, Florianópolis, Brazil, paper MF-103, 2008.
14. L. Consolini, Convective boiling heat transfer in a single micro-channel. Doc. thesis. EPFL, Switzerland, 2008.
15. G. Ribatski, W. Zhang, L. Consolini; J. Xu, J. R. Thome. On the Prediction of Heat Transfer in Micro-Scale Flow Boiling. *Heat Transfer Eng.* vol. 28, pp 842-851, 2007.
16. G. Hetsroni, A. Mosyak, E. Pogrebnyak, and Z. Segal, Explosive Boiling of Water in Parallel Micro-Channels, *Int. J. Multiphase Flow*, vol. 31, pp. 371-392, 2005.
17. L. Consolini, G. Ribatski, Z. Wei, J. Xu, and J.R. Thome, Heat Transfer in Confined Forced Flow-Boiling. *Heat Transfer Engineering*, vol. 28, pp. 826-833, 2007.
18. R.B. Abernethy, and J.W. Thompson, Handbook Uncertainty in Gas Turbine Measurements, Arnold Engineering Development Center, Arnold Air Force Station, Tennessee, 1973.
19. R.J. Moffat, Describing the Uncertainties in Experimental Results, *Exp. Thermal Fluid Sci*., vol. 1, pp. 3-17, 1988.
20. V. Gnielinski, New equations for heat and mass transfer in turbulent pipe and channel from. *Int. Chem. Eng.* vol. pp.16, 359-368, 1976.
21. B. S. Petukhov, in T. F. Irvine and J. P. Hartnett, Eds., *Advances in Heat Transfer*, vol. 6, Academic Press, New York, 1970.
22. Y.-Y. Yan, T.-F. Lin, Evaporation heat transfer and pressure drop of refrigerant R-134a in a small pipe, *Int. J. Heat Mass Transfer,* vol. 41, pp. 4183–4194, 1998.
23. A. A. Arcanjo, J. O. Freitas, C. B. Tibiriça, G. Ribatski. Two-phase flow characteristics during flow boiling of halocarbon refrigerants in micro-scale channels, *ECI International Conference on Boiling Heat Transfer*, Florianópolis, Brazil, May 2009.
24. S. Saitoh, H. Daiguji, E. Hihara, Effect of tube diameter on boiling heat transfer of R-134a in horizontal small-diameter tubes, *International Journal of Heat and Mass Transfer,* vol 48, pp. 4973–4984, 2005.
25. W. Qu and I. Mudawar, Flow boiling heat transfer in two-phase micro-channel heat sinks—II. Annular two phase flow model, *Int. Journal of Heat and Mass* Transfer, vol. 46, pp. 2773–2784, 2003.